

## HARD X-RAY PHOTON INDEX AS AN INDICATOR OF BOLOMETRIC CORRECTION IN ACTIVE GALACTIC NUCLEI

XIN-LIN ZHOU<sup>1,2</sup>, YONG-HENG ZHAO<sup>1,2</sup>

*Draft version November 7, 2018*

### ABSTRACT

We propose the rest-frame 2-10 keV photon index,  $\Gamma_{2-10\text{keV}}$ , acting as an indicator of the bolometric correction,  $L_{\text{bol}}/L_{2-10\text{keV}}$  (where  $L_{\text{bol}}$  is the bolometric luminosity and  $L_{2-10\text{keV}}$  is the rest-frame 2-10 keV luminosity), in radio-quiet active galactic nuclei (AGNs). Correlations between  $\Gamma_{2-10\text{keV}}$  and both bolometric correction and Eddington ratio are presented, based on simultaneous X-ray, UV, and optical observations of reverberation-mapped AGNs. These correlations can be compared with those for high-redshift AGNs to check for any evolutionary effect. Assuming no evolutionary effect in AGNs' spectral properties, together with the independent estimates of  $L_{2-10\text{keV}}$ , the bolometric correction, Eddington ratio, and black hole (BH) mass can all be estimated from these correlations for high-redshift AGNs, with the mean uncertainty of a factor of 2-3. If there are independent estimates of BH masses,  $\Gamma_{2-10\text{keV}}$  for high-redshift AGNs can be used to determine their true  $L_{\text{bol}}$  and  $L_{2-10\text{keV}}$ , and in conjunction with the redshift, can be potentially used to place constraints on cosmology by comparison with the rest-frame 2-10 keV flux. We find that the true  $L_{2-10\text{keV}}$  estimated from  $\Gamma_{2-10\text{keV}}$  for the brightest Type I AGNs with  $z < 1$  in the Lockman Hole is generally in agreement with the observed  $L_{2-10\text{keV}}$ . However, there are still many uncertainties, such as the accurate determination of the intrinsic  $\Gamma_{2-10\text{keV}}$  for distant AGNs and the large uncertainty in the luminosities obtained, which call for significant further study before "AGN cosmology" can be considered a viable technique.

*Subject headings:* sblack hole physics cosmology: observations galaxies: distances and redshifts  
X-rays: diffuse background

### 1. INTRODUCTION

Active galactic nuclei (AGNs) and quasars, as the most powerful long-lasting celestial bodies, are believed to be powered by the accretion of gas onto supermassive black holes (BHs). The cosmological applications of AGNs have long been explored since they have been detected reaching the redshift of  $\sim 6.4$  (Fan et al. 2006). Gunn & Peterson (1965) proposed, using the Ly $\alpha$  resonance absorption in the spectra of distant quasars as a probe for the neutral hydrogen density in the intergalactic medium at high redshift (see the review by Fan et al. 2006). Baldwin (1977) proposed the equivalent width of the C IV line as a luminosity indicator. Since then, many authors studied the correlations between the equivalent width of emission lines and the continuum luminosities (e.g., Shang et al. 2003; Baskin & Laor 2004; Zhou & Wang 2005). However, these correlations show large scatters with uncertain slopes. It is difficult for the equivalent width of emission lines to work as a luminosity indicator.

Although it is difficult to find a simple luminosity indicator for AGNs, one can estimate the true luminosity of an AGN in a distant independent way. This is intriguing since AGNs may potentially become cosmological probes. The bolometric luminosity,  $L_{\text{bol}}$ , of an AGN depends on its BH mass,  $M_{\text{BH}}$ , and Eddington ratio,  $\dot{m}_{\text{E}} \equiv L_{\text{bol}}/L_{\text{Edd}}$ , where  $L_{\text{Edd}}$  is the Eddington luminos-

ity for an AGN's  $M_{\text{BH}}$ . It has been found that the rest-frame 2-10 keV photon index,  $\Gamma_{2-10\text{keV}}$ , is an indicator of  $\dot{m}_{\text{E}}$  (Lu & Yu 1999; Wang et al. 2004; Kelly et al. 2007; Zhou et al. 2007; Shemmer et al. 2008, hereafter S08). If  $M_{\text{BH}}$  can be estimated from a method which is independent of the luminosity, e.g., from the X-ray variability amplitude (Zhou et al. 2010) or the stellar velocity dispersion (Tremaine et al. 2002), the bolometric luminosity of an AGN can be calculated from  $\Gamma_{2-10\text{keV}}$  and  $M_{\text{BH}}$ , under the assumption of no evolutionary effect in AGNs' spectral properties. If the rest-frame 2-10 keV luminosity,  $L_{2-10\text{keV}}$ , can be estimated from  $L_{\text{bol}}$ , we can derive an AGN's luminosity distance by comparison with the absorption-corrected 2-10 keV flux. Therefore, the bolometric correction,  $\kappa_{2-10\text{keV}}$ , defined by the ratio of  $L_{\text{bol}}$  to  $L_{2-10\text{keV}}$ , should also be studied. The previous work on the spectral energy distributions (SEDs) of AGNs suggested that the spread of  $\kappa_{2-10\text{keV}}$  of individual AGNs is large (Elvis et al. 1994). It was found that the optical-to-X-ray SED shape depends on the UV luminosity (e.g., Yuan et al. 1998) and then the dependence of  $\kappa_{2-10\text{keV}}$  on the luminosity is proposed (Marconi et al. 2004). However, Vasudevan & Fabian (2007, hereafter VF07) found that  $\kappa_{2-10\text{keV}}$  is a function of  $\dot{m}_{\text{E}}$ , with no clear dependence on luminosity.

Here we propose  $\Gamma_{2-10\text{keV}}$  to be an indicator of  $\kappa_{2-10\text{keV}}$ . We calibrate the correlations between  $\Gamma_{2-10\text{keV}}/\kappa_{2-10\text{keV}}$ , and  $\Gamma_{2-10\text{keV}}/\dot{m}_{\text{E}}$  based on simultaneous X-ray, UV, and optical observations of low-redshift AGNs with reverberation-based  $M_{\text{BH}}$  (Peterson et al. 2004). These correlations can be used to obtain  $M_{\text{BH}}$  (together with the independent luminosity), or the esti-

zhouxl@nao.cas.cn

<sup>1</sup>Key Laboratory of Optical Astronomy, National Astronomical Observatories, Chinese Academy of Sciences, Beijing, 100012, China

<sup>2</sup>National Astronomical Observatories, Chinese Academy of Sciences, Beijing, 100012, China

mates of an AGN's true luminosity (together with the independent  $M_{\text{BH}}$ ). Throughout this Letter, we assume a cosmology of  $h_0=71 \text{ km s}^{-1} \text{ Mpc}^{-1}$ ,  $\Omega_{\text{m}} = 0.27$ , and  $\Omega_{\Lambda} = 0.73$ .

## 2. SAMPLE AND DATA

Simultaneous X-ray, UV and optical observations of 29 low-redshift ( $z < 0.33$ ) AGNs in Peterson et al.'s (2004) sample obtained from the *XMM-Newton* EPIC and OM instruments have been reduced by Vasudevan & Fabian (2009, hereafter VF09). The purpose of this work is studying  $\Gamma_{2-10\text{keV}}$  as an indicator of  $\kappa_{2-10\text{keV}}$  and  $\dot{m}_{\text{E}}$ , but the beaming emission of radio-loud AGNs may affect the measurements of the intrinsic  $\Gamma_{2-10\text{keV}}$ . Therefore, we remove radio-loud AGNs 3C 120, 3C 390.3, and 3C 273 from this sample. We also remove the quasar PG 1411+442 since this object is heavily obscured. Note that there are a few other sources in the reverberation-mapped sample which, although they may not be heavily absorbed, may have some kind of complex absorption. In those cases it is difficult to really know what the intrinsic  $\Gamma_{2-10\text{keV}}$  is for those objects. VF09 used a broken power-law model to model the 1-8 keV data. This simple approach cannot model the shape of the hard X-ray continuum precisely. Since the whole premise of this work rests on getting good, accurate  $\Gamma_{2-10\text{keV}}$  values for this sample, we take  $\Gamma_{2-10\text{keV}}$  from the more detailed fits available in the literature for the X-ray observations. We present results from 27 observations of 25 AGNs in Table 1.

Most of objects in Table 1 are included in VF07's sample. VF09 compared the shape of the simultaneous SEDs of AGNs in Table 1 with the non-simultaneous SEDs in VF07. The values of  $\dot{m}_{\text{E}}$  and  $\kappa_{2-10\text{keV}}$  obtained in VF09 show a similar range to those in VF07. However,  $\dot{m}_{\text{E}}$  values in Table 1 on average are a factor of  $\sim 0.8$  of VF07's values due to the generally larger  $M_{\text{BH}}$  in Peterson et al. (2004), and  $\kappa_{2-10\text{keV}}$  values in Table 1 are on average  $\sim 1.38$  times larger than VF07's values.

## 3. RESULTS

### 3.1. Photon index and Eddington ratio

We assume that there is a linear correlation,  $y = \alpha + \beta x$ , with the measurement errors of  $\epsilon_{x_i}$  for  $x_i$  and  $\epsilon_{y_i}$  for  $y_i$ . It was shown that the Nukers' estimate is an unbiased slope estimator for the linear regression (Tremaine et al. 2002). The Nukers' estimate is based on minimizing:

$$\chi^2 \equiv \sum_{i=1}^N \frac{(y_i - \alpha - \beta x_i)^2}{\epsilon_{y_i}^2 + \beta^2 \epsilon_{x_i}^2}. \quad (1)$$

Figure 1(a) shows the correlation between  $\Gamma_{2-10\text{keV}}$  and  $\dot{m}_{\text{E}}$  for the present sample. The correlation is significant, with a Spearman's coefficient of 0.55. The Spearman's probability associated with this coefficient is about 0.3%. We then apply the Nukers' estimate using the *fitexy* routine (Press et al. 1992) to derive the correlation between  $\Gamma_{2-10\text{keV}}$  and  $\dot{m}_{\text{E}}$ ,

$$\Gamma_{2-10\text{keV}} = (0.31 \pm 0.02) \log \dot{m}_{\text{E}} + (2.11 \pm 0.02). \quad (2)$$

The minimum  $\chi^2$  per degree of freedom is 21.8, indicating that either the uncertainties on  $\Gamma_{2-10\text{keV}}$  are

underestimated or there is an intrinsic dispersion in the correlation. To account for the intrinsic dispersion in the  $M_{\text{BH}} - \sigma_{\text{rms}}^2$  relation, we replace  $\epsilon_{y_i}$  by  $(\epsilon_{y_i}^2 + \epsilon_0^2)^{1/2}$ , where  $\epsilon_0$  represents the intrinsic dispersion;  $\epsilon_0$  is adjusted so that the value of  $\chi^2$  per degree of freedom is unity. This procedure is preferable if the individual error estimates,  $\epsilon_{y_i}$ , are reliable (Tremaine et al. 2002). Adding an intrinsic dispersion of 0.51 dex decreases the value of  $\chi^2$  per degree of freedom to unity and gives the best-fit result:

$$\log \dot{m}_{\text{E}} = (2.09 \pm 0.58) \Gamma_{2-10\text{keV}} - (4.98 \pm 1.04), \quad (3)$$

as shown in Figure 1(a).

### 3.2. Photon Index and Bolometric Correction

Figure 1(b) shows the correlation between  $\Gamma_{2-10\text{keV}}$  and  $\kappa_{2-10\text{keV}}$ . A Spearman's test returns the correlation coefficient of 0.59, corresponding to the Spearman's probability of 0.1%. We then apply the Nukers' estimate to derive the correlation:

$$\log \kappa_{2-10\text{keV}} = (2.52 \pm 0.08) \Gamma_{2-10\text{keV}} - (3.12 \pm 0.15). \quad (4)$$

The minimum  $\chi^2$  per degree of freedom is 35, indicating that either the uncertainties in  $\kappa_{2-10\text{keV}}$  are underestimated, or there is an intrinsic dispersion in the correlation. We add an intrinsic dispersion of 0.32 dex to decrease the value of  $\chi^2$  per degree of freedom to unity, which gives the best-fit result:

$$\log \kappa_{2-10\text{keV}} = (1.12 \pm 0.30) \Gamma_{2-10\text{keV}} - (0.63 \pm 0.53), \quad (5)$$

as shown in Figure 1(b).

## 4. DISCUSSION

The reverberation-mapped AGNs used here are a subset of AGNs, which are skewed toward moderate luminosity Seyfert 1 galaxies. The bolometric luminosity ranges from  $10^{42.4} \text{ erg s}^{-1}$  to  $10^{46.5} \text{ erg s}^{-1}$ . The Eddington ratio ranges from 0.0004 to 1.13, with a mean value of  $\sim 0.16$ , and only a few AGNs have low values. This is roughly in agreement with a large sample of Seyfert 1 galaxies selected from the Sloan Digital Sky Survey (Figure 12 in Shen et al. 2008).

Equation (2) is in excellent agreement with Equation (1) in S08, which includes high-luminosity AGNs reaching  $z \sim 3.2$ . This suggests that there is no evidence for the evolution of AGNs' spectral properties over cosmological time. Many previous studies suggested that X-ray spectra of high-redshift AGNs (reaching  $z \sim 6$ ) remain similar properties to those of low-redshift ones (e.g., Shemmer et al. 2005). Nevertheless, the spectral bandpass is affected by the redshift. The 2-10 keV band in the observed frame will correspond to energies higher by a factor of  $(1+z)$  in the rest frame. Thus, the rest-frame 2-10 keV band should be used for high-redshift AGNs.

The first idea proposed here is that  $\Gamma_{2-10\text{keV}}$  can be used to estimate  $\dot{m}_{\text{E}}$  and  $\kappa_{2-10\text{keV}}$ , which can then be used along with  $L_{2-10\text{keV}}$  to get  $M_{\text{BH}}$ . A similar possibility was discussed in Zhou et al. (2007) and S08. S08 used the luminosity-dependent  $\kappa_{2-10\text{keV}}$  in Marconi et al. (2004). Note that Marconi et al. (2004) used the nonlinear  $\alpha_{\text{ox}} - L_{2500}$  correlation (e.g., Section 3.3 in S08) to

work out their  $\kappa_{2-10\text{keV}}$ . Here, we use values of  $L_{\text{bol}}$  determined from the SEDs given by the simultaneous X-ray, UV, and optical observations. We find a robust correlation between  $\Gamma_{2-10\text{keV}}$  and  $\kappa_{2-10\text{keV}}$ . This allows the direct estimate of  $\kappa_{2-10\text{keV}}$  from  $\Gamma_{2-10\text{keV}}$ . This significantly extends the work of S08. S08 also argued that this approach can give an estimate of both  $\dot{m}_{\text{E}}$  and  $M_{\text{BH}}$  with mean uncertainties within a factor of  $< 3$ . This is in good agreement with the intrinsic dispersion of correlations derived here. Our best-fitting result of the  $\Gamma_{2-10\text{keV}}-\dot{m}_{\text{E}}$  correlation, Equation (3), is different from Equation (2) in S08. We tend to use our result since the correlation based on reverberation mapped AGNs is more robust.

The second idea proposed here is that  $\Gamma_{2-10\text{keV}}$  can be used, along with an independent measure of  $M_{\text{BH}}$ , to give  $L_{\text{bol}}$  and  $L_{2-10\text{keV}}$ . Note that  $L_{\text{bol}} = \dot{m}_{\text{E}} \times L_{\text{Edd}}$ , where  $L_{\text{Edd}} = 1.26 \times 10^{38} M_{\text{BH}} \text{ erg s}^{-1}$ . Provided the intrinsic  $\Gamma_{2-10\text{keV}}$  is known accurately enough from good quality X-ray data, one can readily get  $L_{\text{bol}}$  from  $\Gamma_{2-10\text{keV}}$  and  $M_{\text{BH}}$ . One can also estimate  $\kappa_{2-10\text{keV}}$  from  $\Gamma_{2-10\text{keV}}$  based on our Equation (5). This allows the direct calculation of  $L_{2-10\text{keV}}$  by using the Equation of  $L_{2-10\text{keV}} = L_{\text{bol}}/\kappa_{2-10\text{keV}}$ . Provided the absorption-corrected rest-frame 2-10 keV flux can be obtained accurately, the luminosity distance can be determined and the AGN becomes a potential cosmological probe.

Figure 2 shows the true  $L_{2-10\text{keV}}$  (open circle) estimated from  $\Gamma_{2-10\text{keV}}$  and  $M_{\text{BH}}$ , compared with the observed  $L_{2-10\text{keV}}$  (filled circle) calculated from the X-ray flux for the brightest Type I AGNs with  $z < 1$  taken from *XMM-Newton* observations of the Lockman Hole (Mateos et al. 2005). The true  $L_{2-10\text{keV}}$  is generally in agreement with the observed  $L_{2-10\text{keV}}$ , with a notable outlier of RDS 426A. This object is very heavily absorbed, with a column density of hydrogen of  $10^{22.09} \text{ cm}^{-2}$  (Mateos et al. 2005).  $M_{\text{BH}}$  is derived from the empirical virial correlation using the  $\text{H}\beta$  or  $\text{Mg II}$  line and the optical luminosity available in Lehmann et al. (2001). The  $M_{\text{BH}}$  estimates mainly depend on the emission-line width, and weakly on the optical continuum luminosity. The second idea requires that  $M_{\text{BH}}$  should be measured from the method independent of the luminosity. The stellar velocity dispersion,  $\sigma_*$ , is an  $M_{\text{BH}}$  estimator independent of luminosity. However, it is difficult to measure  $\sigma_*$  for high-redshift AGNs. Furthermore, there was some evidence for the evolution of the  $M_{\text{BH}} - \sigma_*$  correlation reaching  $z \sim 2$  (Trakhtenbrot & Netzer 2010, and the references therein). Recently, Zhou et al. (2010) suggested that the X-ray variability amplitude (so-called excess variance; Nandra et al. 1997) can act as an indicator of  $M_{\text{BH}}$ . It is also difficult to obtain high-quality X-ray light curves to validate this technique at high redshift.

If there are independent estimates of  $M_{\text{BH}}$  in the future, correlations presented here can also be used to estimate the true luminosity of high-redshift AGNs, which will enable them to be used in a similar way that Type Ia supernovae have been previously used for cosmology applications. AGNs are so ubiquitous in deep X-ray surveys, that their numbers provide significant potential for such work. However, since this method rests on the accurate determination of the intrinsic  $\Gamma_{2-10\text{keV}}$  to get  $\dot{m}_{\text{E}}$  and  $\kappa_{2-10\text{keV}}$ , it will be difficult to get the intrinsic

$\Gamma_{2-10\text{keV}}$  for high-redshift AGNs. For example, in the *Chandra* Deep Fields, only simple hardness ratios can be calculated for many of AGNs, and the steep ratios seen for many of these AGNs indicate that many of them could be heavily absorbed, making it difficult to obtain the intrinsic  $\Gamma_{2-10\text{keV}}$  (Alexander et al. 2003). It is expected that the future International X-ray Observatory, or any other future instruments, will really offer the capabilities to determine  $\Gamma_{2-10\text{keV}}$  sufficiently accurately at higher redshift.

Provided the accurate  $\Gamma_{2-10\text{keV}}$  for high-redshift AGNs can be obtained, the issue still remains that an AGN's luminosity varies significantly over even short timescales. The correlations presented here can be used for the luminosity estimates, but the uncertainty inherent in these correlations would be just as big as a stumbling block to doing cosmology. Assuming that the error of  $M_{\text{BH}}$  is 0.3 dex, assuming  $\Gamma_{2-10\text{keV}}$  comes with an error of  $\pm 0.2$ , the error of luminosity estimates from these correlations is  $\sim 0.37$ . This is just the lower limit of actual one due to the X-ray variability, since the X-ray flux- $\Gamma_{2-10\text{keV}}$  correlation exhibits an inverted behaviour for an AGN (Figure 9 in Ponti et al. 2006). The error of  $M_{\text{BH}}$  may be underestimated for high-redshift objects. This further enlarges the uncertainty in the luminosity obtained. Therefore, it is difficult to give useful constraints on cosmology with the AGN data. The refined versions of the correlations would need to be produced in future with cleaner objects.

## 5. CONCLUSIONS

Correlations between hard X-ray photon index and both bolometric correction and Eddington ratio are presented, based on simultaneous X-ray, UV, and optical observations of radio-quiet AGNs with reverberation-based BH masses. We thus propose X-ray photon index acting as an indicator of bolometric correction. Assuming no evolutionary effect of AGNs' spectral properties, together with the X-ray luminosity, the bolometric correction, Eddington ratio, and BH mass can all be estimated from these correlations for the high-redshift AGNs, with the mean uncertainty within a factor of 2-3.

With the BH mass known to be independent of the luminosity, the true luminosity of an AGN can be calculated from its X-ray photon index based on the correlations presented here. We find that the true X-ray luminosity estimated from the photon index for the brightest Type I AGNs with  $z < 1$  in the Lockman Hole is generally in agreement with the observed X-ray luminosity. However, the errors of AGNs' luminosity estimates depend on the various uncertainties in the X-ray spectra, variability, and some unknown systematic effects in the distant BH mass estimates, which is too much to get an accurate estimate of the cosmology.

We acknowledge the two referees for many useful comments to improve the manuscript significantly. James Wicker is thanked for improving English. This work is supported by the Guoshoujing Telescope (formerly named the Large Sky Area Multi-Object Fiber Spectroscopic Telescope - (LAMOST)), which is funded by the National Development and Reform Commission, operated and managed by the Key Laboratory of Optical As-

tronomy, NAOC. This research has made use of observations obtained with *XMM-Newton*, an ESA science mis-

sion with instruments and contributions directly funded by ESA member states and NASA, USA.

## REFERENCES

- Alexander, D. M. et al. 2003, *AJ*, 126, 539  
 Baldwin, J. A. 1977, *ApJ*, 214, 679  
 Baskin, A., & Laor, A. 2004, *MNRAS*, 350, L31  
 Brinkmann, W., Grupe, D., Branduardi-Raymont, G., & Ferrero, E. 2003, *A&A*, 398, 81  
 Blustin, A. J. et al. 2003, *A&A*, 403, 481  
 D'Ammando, F., Bianchi, S., Jiménez-Bailón, E., & Matt, G. 2008, *A&A*, 482, 499  
 Dasgupta, S., & Rao, A. R. 2006 *ApJ*, 651, 13  
 Denney, K. D. et al. 2006, *ApJ*, 653, 152  
 Elvis, M. et al. 1994, *ApJS*, 95, 1  
 Fan, X., Carilli, C. L., & Keating, B. 2006, *ARA&A*, 44, 415  
 Gallo, L. C., Fabian, A. C., Boller, T., & Pietsch, W. 2005, *MNRAS*, 363, 64  
 Gondoin, P., Orr, A., Lumb, D., & Santos-Lleó, M. 2002, *A&A*, 388, 74  
 Gondoin, P., Lumb, D., Siddiqui, H., Guainazzi, M., & Schartel, N. 2001, *A&A*, 373, 805  
 Gondoin, P., Orr, A., Lumb, D., & Siddiqui, H. 2003, *A&A*, 397, 883  
 Grier, C. et al. 2008, *ApJ*, 688, 837  
 Gunn, J. E., & Peterson, B. A. 1965, *ApJ*, 142, 1633  
 Inoue, H., Terashima, Y., & Ho, L. C. 2007, *ApJ*, 662, 860  
 Kelly, B. C., Bechtold, J., Siemiginowska, A., Aldcroft, T., & Sobolewska, M., 2007, *ApJ*, 657, 116  
 Lehmann, I. et al. 2001, *A&A*, 371, 833  
 Lu, Y. J., & Yu, Q. J. 1999, *ApJ*, 526, L5  
 Marconi A., Risaliti G., Gilli R., Hunt L. K., Maiolino R., & Salvati M., 2004, *MNRAS*, 351, 169  
 Mateos, S., Barcons, X., Carrera, F. J., Ceballos, M. T., Hasinger, G., Lehmann, I., Fabian, A. C., & Streblyanska, A. 2005, *A&A*, 444, 79  
 Markowitz, A., Reeves, J. N., George, I. M., Braito, V., Smith, R., Vaughan, S., Arvalo, P., & Tombesi, F. 2009, *ApJ*, 691, 922  
 Nandra K., George I. M., Mushotzky R. F., Turner T. J., & Yaqoob T., 1997, *ApJ*, 476, 70  
 Page, K. L., Schartel, N., Turner, M. J. L., & O'Brien, P. T. 2004, *MNRAS*, 352, 523  
 Peterson, B. M. et al. 2004, *ApJ*, 613, 682  
 Reeves, J. N., Nandra, K., George, I. M., Pounds, K. A., Turner, T. J., & Yaqoob, T. 2004, *ApJ*, 602, 648  
 Reeves, J. N., Pounds, K., Uttley, P., Kraemer, S., Mushotzky, R., Yaqoob, T., George, I. M., & Turner, T. J. 2005, *ApJ*, 633, 81  
 Piconcelli, E., Jimenez-Bailón, E., Guainazzi, M., Schartel, N., Rodríguez-Pascual, P. M., & Santos-Lleó, M. 2005, *A&A*, 432, 15  
 Ponti, G., Miniutti, G., Cappi, M., Maraschi, L., Fabian, A. C., & Iwasawa, K. 2006, *MNRAS*, 368, 903  
 Ponti, G. et al. 2009, *MNRAS*, 394, 1487  
 Press, W. H., Teukolsky, S. A., Vetterling, W. T., & Flannery, B. P. 1992, *nrfa.book*, Numerical Recipes in FORTRAN: The Art of Scientific Computing (2d ed.; Cambridge: Cambridge Univ. Press)  
 Shang, Z. H., Wills, B. J., Robinson, E. L., Wills, D., Laor, A., Xie, B., & Yuan, J. 2003, *ApJ*, 586, 52  
 Shemmer, O., Brandt, W. N., Netzer, H., Maiolino, R., & Kaspi, S. 2008, *ApJ*, 682, 93 (S08)  
 Shemmer, O., Brandt, W. N., Vignali, C., Schneider, D. P., Fan, X., Richards, G. T., & Strauss, Michael A. 2005, *ApJ*, 630, 729  
 Shen, Y., Greene, J. E., Strauss, M. A., Richards, G. T., & Schneider, D. P. 2008, *ApJ*, 680, 169  
 Steenbrugge, K. C. et al. 2003, *A&A*, 408, 921  
 Trakhtenbrot, B., & Netzer, H. 2010, *MNRAS*, 406, L35  
 Tremaine, S. et al. 2002, *ApJ*, 574, 740  
 Vaughan, S., Fabian, A. C., Ballantyne, D. R., De Rosa, A., Piro, L., & Matt, G. 2004, *MNRAS*, 351, 193  
 Vasudevan, R. V., & Fabian, A. C. 2007, *MNRAS*, 381, 1235 (VF07)  
 Vasudevan, R. V., & Fabian, A. C. 2009, *MNRAS*, 392, 1124 (VF09)  
 Wang, J. M., Watarai, K. Y., & Mineshige, S. 2004, *ApJ*, 607, 107  
 Yuan, W., Brinkmann, W., Siebert, J., & Voges, W. 1998, *A&A*, 330, 108  
 Zhou, X. L., Zhang, S. N., Wang, D. X., & Zhu, L. 2010, *ApJ*, 710, 16  
 Zhou, X. L., & Zhang, S. N. 2010, *ApJ*, 713, L11  
 Zhou, X. L., & Wang, J. M. 2005, *ApJ*, 618, L83  
 Zhou, X. L., Yang, F., Lv, X. R., & Wang, J. M. 2007, *AJ*, 133, 432

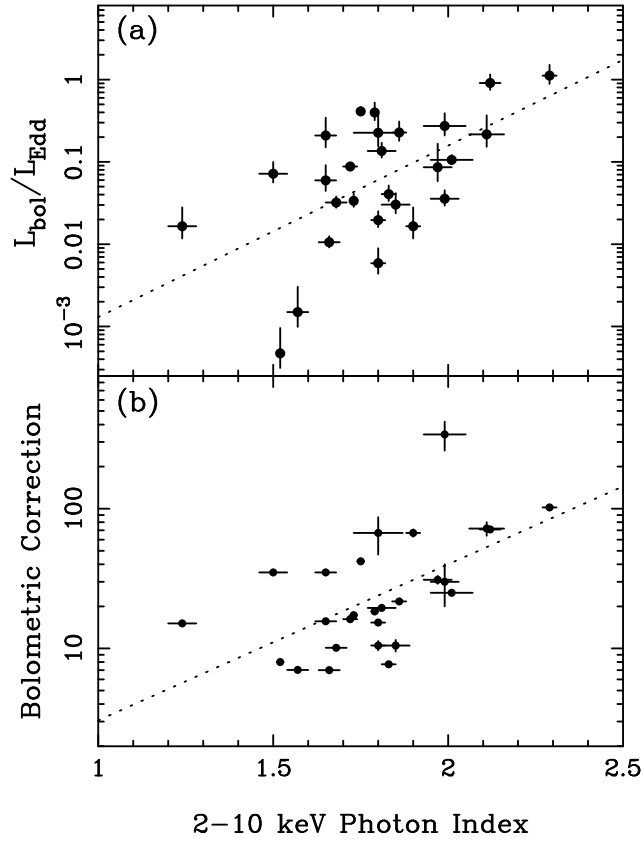


FIG. 1.— Panel (a): Correlation between  $\Gamma_{2-10\text{keV}}$  and  $\dot{m}_{\text{E}}$ . The dotted line denotes the best fitting result of Equation (3); Panel (b): Correlation between  $\Gamma_{2-10\text{keV}}$  and  $\kappa_{2-10\text{keV}}$ . The dotted line denotes the best fitting result of Equation (5).

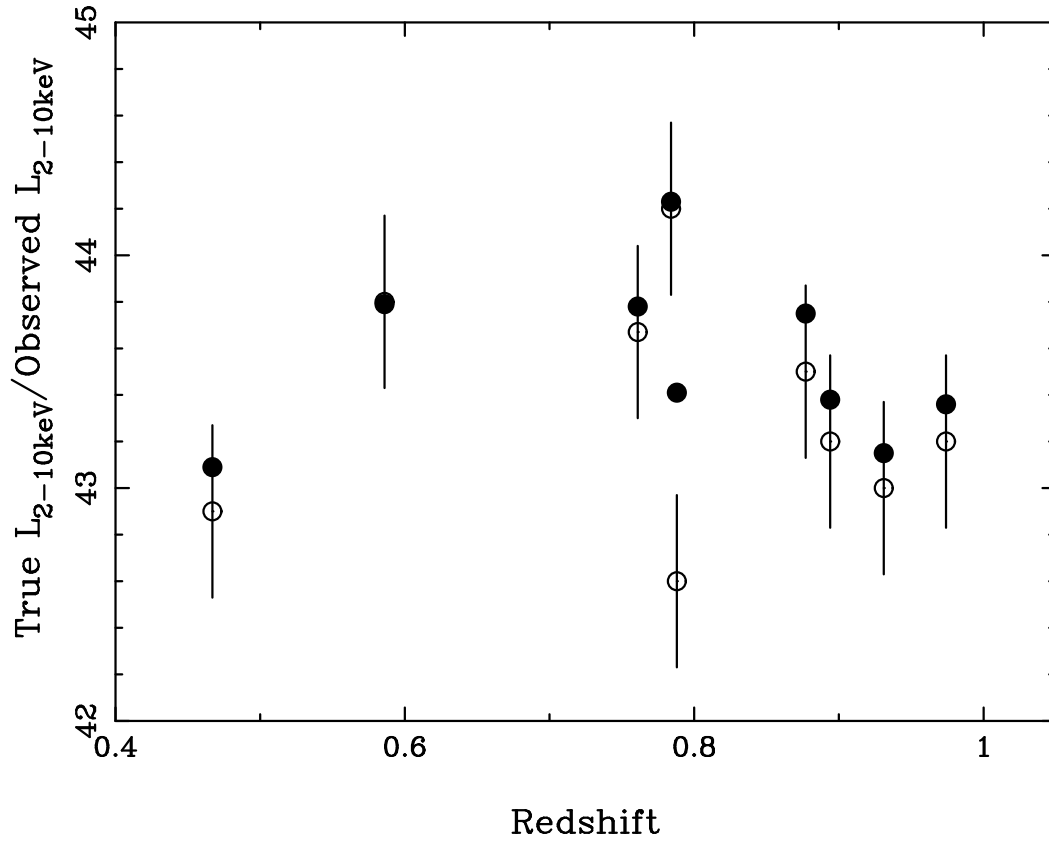


FIG. 2.— True  $L_{2-10\text{keV}}$  (open circle) estimated from  $\Gamma_{2-10\text{keV}}$  and  $M_{\text{BH}}$ , compared with the observed  $L_{2-10\text{keV}}$  (filled circle) calculated from the X-ray flux for the brightest Type I AGNs with  $z < 1$  taken from *XMM-Newton* observations of the Lockman Hole. The true  $L_{2-10\text{keV}}$  is generally in agreement with the observed  $L_{2-10\text{keV}}$ .  $M_{\text{BH}}$  is derived from the empirical virial correlation, which mainly depends on the emission-line width and weakly on the continuum luminosity.

TABLE 1. LOW-REDSHIFT RADIO-QUIET AGNs WITH REVERBERATION-BASED MASS

Name (1)	$M_{\text{BH}}$ (2)	$\Gamma_{2-10\text{keV}}$ (3)	$L_X$ (4)	$L_{\text{bol}}$ (5)	$\dot{m}_{\text{E}}$ (6)	$\kappa_{2-10\text{keV}}$ (7)	$L_X/L_{\text{Edd}}$ (8)	ref. (9)
Mrk 335	$14.2 \pm 3.7$	$2.29 \pm 0.02$	43.3	45.3	1.13	$102^{+4}_{-4}$	-1.95	1
PG 0052+251	$369 \pm 76$	$1.81 \pm 0.04$	44.6	45.8	0.148	$19.5^{+0.7}_{-0.6}$	-2.07	2
F9	$255 \pm 56$	$1.80 \pm 0.02$	43.8	44.8	0.0186	$10.5^{+0.8}_{-0.8}$	-2.71	3
Mrk 590	$47.5 \pm 7.4$	$1.66 \pm 0.03$	43.0	43.8	0.0104	$7.0^{+0.2}_{-0.2}$	-2.68	4
Akn 120	$150 \pm 19$	$2.01 \pm 0.06$	43.9	45.3	0.111	$25.0^{+0.2}_{-0.3}$	-2.38	5
Mrk 79	$52.4 \pm 14.4$	$1.85 \pm 0.04$	43.3	44.3	0.0309	$10.5^{+1.0}_{-0.9}$	-2.52	6
PG 0844+349	$92.4 \pm 38.1$	$2.11 \pm 0.05$	43.6	45.4	0.233	$72^{+8}_{-8}$	-2.47	7
Mrk 110	$25.1 \pm 6.1$	$1.79 \pm 0.01$	43.9	45.1	0.433	$18.4^{+0.1}_{-0.1}$	-1.60	8
PG 0953+414	$276 \pm 59$	$2.12 \pm 0.03$	44.7	46.5	0.892	$71^{+2}_{-2}$	-1.84	9
NGC 3227 (1)	$42.2 \pm 21.4$	$1.57 \pm 0.03$	42.1	42.9	0.00151	$7.02^{+0.05}_{-0.05}$	-3.63	10
NGC 3227 (2)	$42.2 \pm 21.4$	$1.52 \pm 0.01$	41.5	42.4	0.000447	$8.0^{+0.1}_{-0.1}$	-4.23	11
NGC 3516	$42.7 \pm 14.6$	$1.80 \pm 0.02$	42.3	43.5	0.00612	$15.32^{+0.10}_{-0.10}$	-3.43	4
NGC 3783	$29.8 \pm 5.4$	$1.73 \pm 0.01$	42.9	44.1	0.0363	$17.3^{+0.2}_{-0.2}$	-2.67	12
NGC 4051 (1)	$1.91 \pm 0.78$	$1.90 \pm 0.02$	40.8	42.6	0.0164	$67^{+4}_{-3}$	-3.58	13
NGC 4051 (2)	$1.91 \pm 0.78$	$1.24 \pm 0.04$	41.4	42.6	0.0151	$15.1^{+0.2}_{-0.1}$	-2.98	13
NGC 4151	$13.3 \pm 4.6$	$1.65 \pm 0.03$	42.8	44.0	0.0558	$15.64^{+0.08}_{-0.08}$	-2.42	4
PG 1211+143	$146 \pm 44$	$1.99 \pm 0.06$	43.2	45.7	0.260	$340^{+80}_{-60}$	-3.06	14
PG 1229+204	$73.2 \pm 35.2$	$1.97 \pm 0.04$	43.4	44.9	0.0823	$31^{+2}_{-2}$	-2.56	2
NGC 4593	$9.8 \pm 2.1$	$1.83 \pm 0.02$	42.8	43.7	0.0369	$7.7^{+0.1}_{-0.1}$	-2.03	15
PG 1307+085	$440 \pm 123$	$1.50 \pm 0.04$	44.0	45.6	0.0659	$35^{+1}_{-1}$	-2.74	9
Mrk 279	$34.9 \pm 9.2$	$1.86 \pm 0.02$	43.6	45.0	0.210	$21.7^{+0.3}_{-0.3}$	-2.04	4
NGC 5548	$49.4 \pm 7.7$	$1.68 \pm 0.03$	43.3	44.3	0.0236	$10.1^{+0.1}_{-0.1}$	-2.49	4
PG 1426+015	$886 \pm 187$	$1.99 \pm 0.04$	44.1	45.6	0.0243	$30^{+40}_{-10}$	-2.95	16
PG 1613+658	$279 \pm 129$	$1.80 \pm 0.07$	44.1	45.9	0.221	$67^{+20}_{-10}$	-2.45	9
Mrk 509	$143 \pm 12$	$1.72 \pm 0.02$	44.0	45.2	0.0951	$16.20^{+0.10}_{-0.09}$	-2.26	17
PG 2130+099	$38 \pm 15$	$1.65 \pm 0.03$	43.5	45.0	0.0179	$35^{+1}_{-1}$	-2.18	18
NGC 7469	$12.2 \pm 1.4$	$1.75 \pm 0.01$	43.2	44.8	0.369	$42^{+1}_{-1}$	-1.99	19

(1) Object name. (2) Black hole mass, in units of  $10^6 M_{\odot}$ , taken from Peterson et al. (2004), except for NGC 4593 (Denney et al. 2006) and PG 2130+099 (Grier et al. 2008). (3) Rest-frame 2-10 keV photon index. (4) Rest-frame 2-10 keV luminosity. (5) Bolometric luminosity. (6) Eddington ratio,  $\dot{m}_{\text{E}} \equiv L_{\text{bol}}/L_{\text{Edd}}$ . (7) Bolometric correction,  $\kappa_{2-10\text{keV}} \equiv L_{\text{bol}}/L_{2-10\text{keV}}$ . (8) Ratio of rest-frame 2-10 keV luminosity to the Eddington luminosity. (9) Reference for the X-ray observation. (1) Gondoin et al. (2002); (2) D'Ammando et al. (2008); (3) Gondoin et al. (2001); (4) Zhou & Zhang (2010); (5) Vaughan et al. (2004); (6) Gallo et al. (2005); (7) Brinkmann et al. (2003); (8) Dasgupta & Rao (2006); (9) Piconcelli et al. (2005); (10) Markowitz et al. (2009); (11) Gondoin et al. (2003); (12) Reeves et al. (2004); (13) Ponti et al. (2006); (14) Reeves et al. (2005); (15) Steenbrugge et al. (2003); (16) Page et al. (2004); (17) Ponti et al. (2009); (18) Inoue et al. (2007); (19) Blustin et al. (2003).